

1 Electronic Supplementary Information for

2 **Electrospun flexible self-standing Cu-Al₂O₃ fibrous membranes as**
3 **Fenton catalysts for bisphenol A degradation**

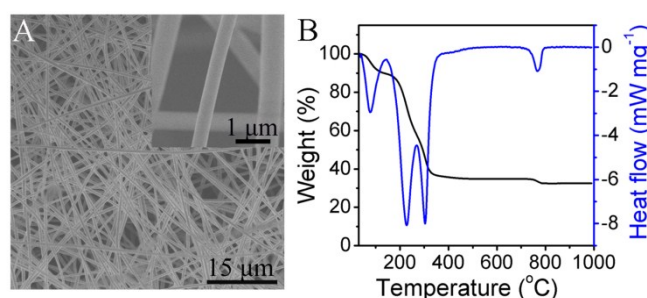
4 Yan Wang^a, Jiang Li^{a, b}, Jianyang Sun^a, Yanbin Wang^a, Xu Zhao^{*a, c}

5 a, Key Laboratory of Drinking Water Science and Technology, Research Center for Eco-
6 Environmental Sciences, Chinese Academy of Sciences, Beijing 100085, P.R. China.

7 b, School of Light Industry and Chemical Engineering, Dalian Polytechnic University, Dalian
8 116034, P. R. China

9 c, University of Chinese Academy of Sciences, Beijing, P.R. China.

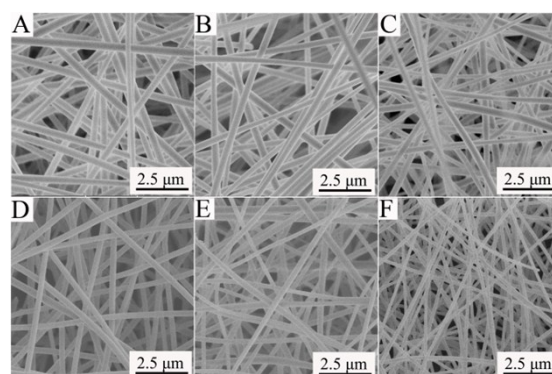
10



11

12 **Fig. S1** (A) SEM image and (B) TG-DSC curves of the 5 wt% Cu-Al₂O₃ xerogel fibrous membranes

13



14

15 **Fig. S2** SEM images of Cu-Al₂O₃ membranes. (A-D) Cu-Al₂O₃-600 membranes with various Cu
16 content (A) 1 wt%, (B) 3 wt%, (C) 5 wt%, (D) 7 wt%; (E-F) 5 wt% Cu-Al₂O₃ membranes calcined
17 at various temperatures (E) 700 °C, (F) 800 °C.

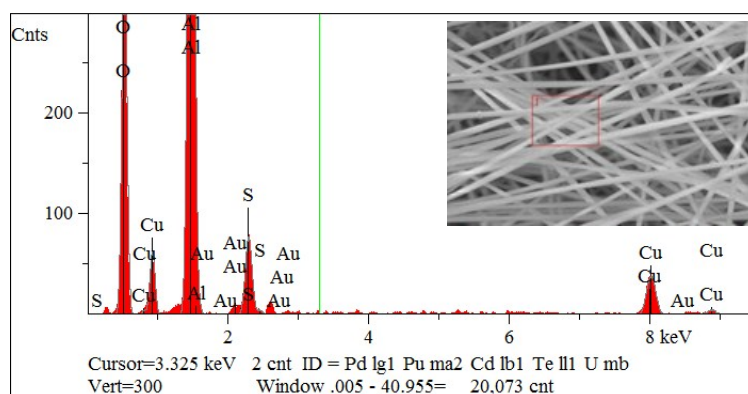


Fig. S3 EDS of 5 wt% Cu-Al₂O₃-600 membranes.

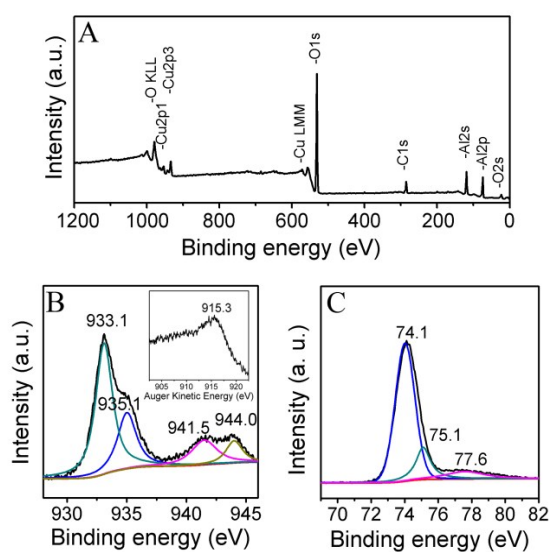


Fig. S4 XPS analysis of the 5 wt% Cu-Al₂O₃-800 membrane, (A) XPS survey (B) Cu 2p and (C) Al 2p spectra.

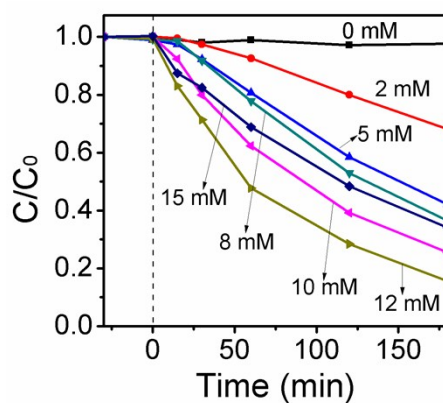


Fig. S5 The influence of H₂O₂ dosage on the BPA degradation by the 5 wt% Cu-Al₂O₃-600 membrane. Conditions: [BPA] = 20 mg/L, initial pH 7.

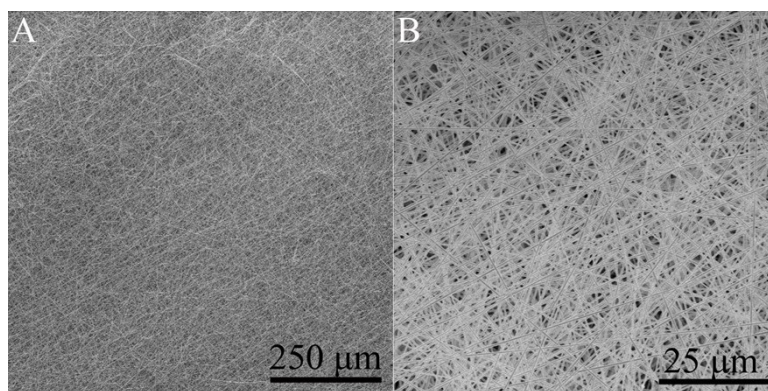


Fig. S6 (A) low magnification and (B) high magnification SEM images of the membrane after the continuous degradation reactions.

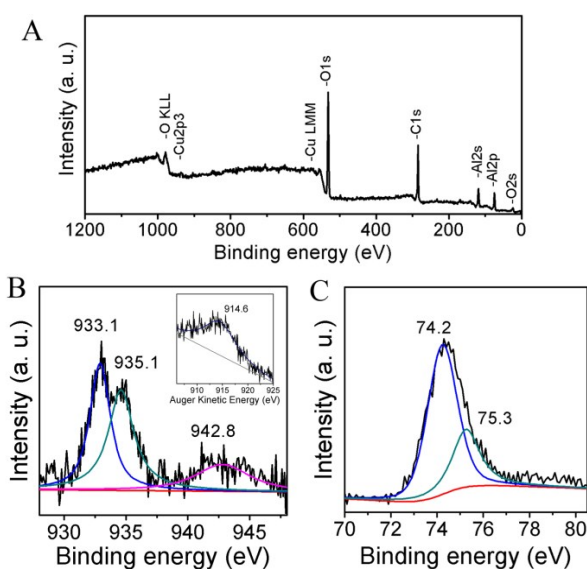


Fig. S7 XPS analysis of the 5% Cu-Al₂O₃-600 membrane after use, (A) XPS survey (B) Cu 2p and (C) Al 2p spectra.

Table. S1 Average fiber diameter of various Cu-Al₂O₃ samples

Sample	Average fiber diameter (nm)	Sample	Average fiber diameter (nm)
1 wt% -600 °C	390	7 wt% -600 °C	320
3 wt% -600 °C	360	5 wt% -700 °C	270
5 wt% -600 °C	340	5 wt% -800 °C	190

Table. S2 Elemental composition of 5 wt% Cu–Al₂O₃-600 membranes.

Elements	Intensity (c/s)	Atomic (%)	Concentration (wt.%)
O	173.45	57.856	42.88
Al	600.93	37.173	46.47
Cu	32.47	2.237	6.59
S	46.81	2.735	4.06
Total		100.00	100.00

Table S3 The BET surface areas and porosity of the samples

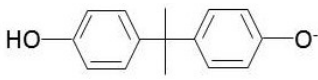
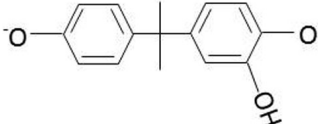
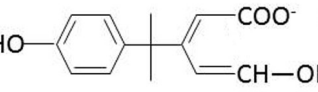
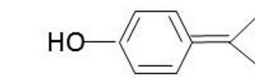
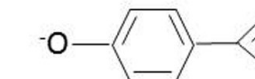
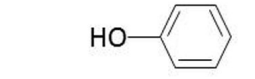
Samples	BET surface area (m ² g ⁻¹)	Pore width (nm)	Pore volume (cc g ⁻¹)
1 wt% Cu-Al ₂ O ₃ -600	12.33	5.75	0.01930
3 wt% Cu-Al ₂ O ₃ -600	9.26	6.22	0.01175
5 wt% Cu-Al ₂ O ₃ -600	10.10	5.92	0.01588
7 wt% Cu-Al ₂ O ₃ -600	8.11	5.19	0.01278
5 wt% Cu-Al ₂ O ₃ -700	40.56	5.44	0.07532
5 wt% Cu-Al ₂ O ₃ -800	38.63	5.51	0.07347

Table S4 Results of Fenton-like degradation of BPA based on various Cu-based catalysts

Catalyst	morphology	BPA initial conc. (ppm)	H ₂ O ₂ initial concentration (mM)	Removal ability	Ref.
copper–aluminum– silica	nanospheres	23	10	98.3% within 60 min	[1]
Mesoporous γ-Cu-Al ₂ O ₃	powders	23	10	100% within 180 min	[2]
Mesoporous Cu/TUD-1	powders	100	90	90.4% within 180 min	[3]
1 wt% Cu- Al ₂ O ₃ -600 °C	membranes	20	12	87% within 180 min	This work
5 wt% Cu- Al ₂ O ₃ -800 °C	membranes	20	12	85% within 60 min	This work

Reaction conditions: catalyst concentration 1.0 g L⁻¹, Initial pH 7 (except for Mesoporous Cu/TUD-1, Initial pH 3.5).

Table S5 Identification of the intermediates by UPLC-Q-TOF-MS.

Products	Structure	m/z
BPA		227
P1		242
P2		247
P3		135
P4		133
P5		94
P6	$\text{HOOC-CH}_2\text{-CH}_2\text{-COO}^-$	117
P7	HOOC-CH=CH-COO^-	115
P8	$\text{H-C(=O)-CH=CH-COO}^-$	99
P9	OOC-CH(OH)-CH_3	89

The XPS spectra of the 5 wt% Cu-Al₂O₃ membrane calcined at 800 °C was shown in Fig. S4. In the XPS survey spectrum, the peaks of Al, O, Cu, and C elements are observed, while the peaks of S element are absence. The results indicate that SO₄²⁻ is totally removed when the membrane calcined at 800 °C. In the Cu 2p and Al 2p XPS spectra, both of Cu⁺ (933.1 eV), Cu²⁺ (935.1 eV) and Al-O-Al (74.1 eV), Al-O-Cu (75.1 eV) are observed. The shakeup satellite line at 941.5 and 944.0 eV in Cu 2p_{3/2} spectra correspond to Cu²⁺.⁴ The auger kinetic energy at 915.3 eV in AES spectra confirmed the

1 existence of Cu^+ , and 77.6 eV in Al 2p spectra was assigned to Al^{3+} .⁵

2
3 The details of the methods for preparing Cu- Al_2O_3 catalysts are discussed as follows: In the
4 literature, the Cu- Al_2O_3 catalyst is usually prepared by a two-step procedure.^{6,7} Specifically, the first
5 step is the preparation of Al_2O_3 powder through evaporation-induced self-assembly method, which is
6 used as the catalyst support; in the second step, the Cu- Al_2O_3 powder catalyst is prepared by
7 immersing Al_2O_3 powder in to the copper precursor such as $\text{Cu}(\text{NO}_3)_2 \cdot 3\text{H}_2\text{O}$, which is called
8 impregnation method, and it is usually followed by a calcination procedure. The two-step preparation
9 method usually resulted in the powder form catalyst, and the Cu catalyst is easy to drop off from the
10 Al_2O_3 support.

11 In some research, the Cu- Al_2O_3 catalyst is prepared by a one-step procedure via the
12 evaporation-induced self-assembly method followed by a calcination procedure.² This method could
13 obtain the Cu- Al_2O_3 catalyst with Al-O-Cu bond, which could decrease the Cu leaching during use.
14 However, the Cu- Al_2O_3 catalyst obtained by this method is still in powder form, and evaporation-
15 induced self-assembly method usually need a long time to evaporate the solvents.

16 In this paper, the Cu- Al_2O_3 catalyst is prepared by a one-step procedure via electrospinning
17 method. The copper is dissolved in the alumina precursor, and the Cu- Al_2O_3 membrane catalyst
18 could be directly obtained via the electrospinning process followed by a calcination procedure.
19 During the electrospinning process, the solvent evaporate rapidly, leading to the immediately
20 formation of Cu- Al_2O_3 nanofibers with uniformly distributed Al-O-Cu bond in the fibers. The high
21 aspect ratio of the nanofibers is good for the formation of flexible Cu- Al_2O_3 membranes.

22
23
24 Because the H_2O_2 dosage is a key factor that influence the Fenton reaction,² the reaction was
25 optimized by varying the H_2O_2 dosage. As shown in Fig. S5, the removal percentages of BPA within
26 3 h were 3%, 32%, 58%, 64%, 75%, 84% and 67% when the H_2O_2 dosages were 0, 2, 5, 8, 10, 12
27 and 15 mM, respectively. The degradation rate increased when the H_2O_2 dosages increased from 0-
28 12 mM, because $\cdot\text{OH}$ is generated by the H_2O_2 precursor. However, the degradation rate decreased
29 when the H_2O_2 dosages increased from 12 mM to 15 mM, and this is supposed to be caused by the
30 scavenging effect of $\cdot\text{OH}$ by excess H_2O_2 .² Therefore, 12 mM was the optimal H_2O_2 dosage in this
31 reaction.

The leaching percentages of Cu and Al in the membranes are calculated. The computation process is as follows: for the 1 wt% Cu-Al₂O₃, the amount of Cu in 10 mg membrane is 0.1 mg; After reaction, Cu leaching is 0.151 mg L⁻¹, the reaction solution is 10 mL, thus the amount of Cu leaching is 0.151 mg/L*0.01 L=0.00151 mg; the percentage of Cu leaching is 0.00151/0.1=1.51% for the 1 wt% Cu-Al₂O₃ membrane. Hence, for 1, 3, 5, 7 wt% Cu-Al₂O₃ membranes, the Cu leaching percentages are respectively 1.51%, 0.43%, 0.64%, 0.61%, and the Al leaching percentages are all remained 0.02%.

Fig. S7 presents the XPS results of the Cu-Al₂O₃-600 membrane after use. It can be seen that the peaks of the main elements of the membranes including Al, O, and Cu are observed in the XPS survey spectrum. From the Cu 2p and Al 2p spectra, it can be seen that the peaks of the Cu⁺ (933.1 and 914.6 eV), Cu²⁺ (935.1 and 942.8 eV), Al-O-Al (74.2 eV) and Al-O-Cu (75.3 eV) are all exhibited.

The intermediates of BPA degradation were identified by UPLC-Q-TOF-MS. As shown in Table S5, there were nine intermediates (formulated from P1 to P9) besides BPA itself. The P1 (m/z 242), P2 (m/z 247), P3 (m/z 135), P4 (m/z 133), and P5 (m/z 94) were identified to be the intermediates that still possess aromatic ring; The P6 (m/z 117), P7 (m/z 115), P8 (m/z 99), and P9 (m/z 89) were identified to be the intermediates that after the ring-opening reactions. These intermediates were generally in agreement with those in previous reports.^{8,9}

References

- [1] L. Lyu, L. Zhang, C. Hu, M. Yang, *J. Mater. Chem. A* 2016, **4**, 8610-8619.
- [2] L. Lyu, L. Zhang, Q. Wang, Y. Nie and C. Hu, *Environ. Sci. Technol.*, 2015, **49**, 8639-8647.
- [3] M. P. Pachamuthu, S. Karthikeyan, R. Maheswari, A. F. Lee and A. Ramanathan, *Appl. Surf. Sci.* 2017, **393**, 67-73.
- [4] F. Parmigiani, G. Pacchioni, F. Illas, P.S. Bagus, *J Electron Spectrosc.* 1992, **592**, 55-269.
- [5] J.R. Lindsay, H.J. Rose, W.E. Swartz, P.H. Watts, K.A. Rayburn, *Appl. Spectrosc.* 1973, **27**, 1-5.
- [6] L. Li, W. Han, F. Dong, L. Zong, Z. Tang and J. Zhang, *Micropor. Mesopor. Mater.*, 2017, **249**, 1-9.

- 1 [7] I. Obregón, I. Gandarias, A. Ocio, I. García-García, N. Alvarez de Eulate and P. L. Arias, *Appl.*
2 *Catal. B-Environ.*, 2017, **210**, 328-341.
- 3 [8] J. Sharma, I. M. Mishra, D. D. Dionysiou and V. Kumar, *Chem. Eng. J.*, 2015, **276**, 193-204.
- 4 [9] J. Zhang, B. Sun and X. Guan, *Sep. Purif. Technol.*, 2013, **107**, 48-53.